Kinetic length, step permeability, and kinetic coefficient asymmetry on the Si(111) (7×7) surface

W. F. Chung and M. S. Altman*
Department of Physics, Hong Kong University of Science and Technology, Kowloon, Hong Kong
(Received 30 May 2002; published 30 August 2002)

The island nucleation position at the critical terrace width for step flow on the Si(111) (7×7) surface has been measured with low-energy electron microscopy. These data allow for the kinetic length, which is indicative of the rate-limiting step, to be evaluated and provide compelling new evidence that steps are impermeable. The assessment of step kinetic coefficient asymmetry and its potential for effecting growth instabilities depends crucially upon the kinetic length and step permeability. Step attachment is found to be favored from the terrace trailing an advancing step.

DOI: 10.1103/PhysRevB.66.075338 PACS number(s): 68.35.Fx, 68.37.Nq, 68.43.Jk, 68.55.Ac

Step flow and two-dimensional island nucleation and growth (2DNG) are two of the basic mechanisms of crystal growth.[1] The resulting growth morphologies are strongly influenced by the kinetics of surface diffusion and incorporation of atoms into the condensed phase by step attachment. Asymmetric step attachment is recognized to be an important and possibly common cause of growth instabilities, particularly in step flow.[2–8] The most commonly cited reason for asymmetric step attachment kinetics is the presence of a Schwoebel-Ehrlich diffusion energy barrier at a step.[2,9] However, asymmetric step attachment is important in the context of growth instabilities only if it causes the current densities to a step from the adjacent terraces to be unequal. It will be shown explicitly below that the realization of asymmetric current density may be hindered in real systems by other factors such as step permeability and the relative importance of diffusion and step attachment, i.e., the rate limiting step, which is characterized in the extremes as diffusion limited (DL) and attachment/detachment limited (ADL). For this reason, it is essential to consider the rate limiting step and permeability on an equal footing as step attachment asymmetry.

In this paper, we examine the kinetics of step attachment on the Si(111) (7×7) surface. Despite being one of the most widely studied crystal surfaces, several aspects of diffusion, step attachment, and permeability either remain unclear or are only just emerging. Previously, comparison of denuded zones at the upper and lower sides of steps provided no evidence for a reflective Schwoebel-Ehrlich barrier at the upper sides of steps.[10] However, the presence of such a barrier to descending diffusive motion was inferred from the comparison of the decay of two-dimensional islands and holes.[11] The fact that islands and holes were observed to decay at different rates was also taken as evidence of ADL processes.[11] This view was supported by recent analysis of the decay rates of mounds.[12]

The problem is addressed here by examining the transition between step flow and 2DNG. The island nucleation position at the critical terrace width is used as a probe of the steady-state, nonequilibrium adatom concentration on a terrace during growth. Comparison is made to concentrations that are derived from solution of the diffusion equation subject to realistic boundary conditions that take step attachment asymmetry and step permeability into account. This comparison indicates that growth occurs intermediate between step attachment and detachment and diffusion limited regimes. Compelling new evidence is also obtained that steps are impermeable, which is surprising considering that it takes the concerted action of many atoms to attach in the form of the (7×7) structure at a step edge. Step kinetic coefficient asymmetry is also found that favors attachment from the terrace trailing an advancing step, which has not been observed previously.

The experiments were carried out in a low energy electron microscope (LEEM) with base pressure of 1×10^{-10} Torr. The sample had a nominal miscut of 0.1° from the (111) direction. Doping was *n*-type (phosphorous) with resistivity 10 Ohm-cm. The sample was heated by electron bombardment from the rear. The sample was intentionally cooled very slowly through the (1×1) to (7×7) phase transition in order to obtain domains that spanned the terraces. Deposition was made from an electron beam heated Si rod. The absolute flux calibration was made by direct observation of the growth rate using LEEM. The imaging principle and real-time capability of LEEM have been described previously.[13] A quantitative wave-optical model for step contrast has been developed which allows for the routine identification of the up and down sides of a step by visual inspection of the step contrast details and for determining the step position precisely.[14] In particular, a bright interference fringe appears on the lower (i.e., leading terrace) side of a step in underfocus for the imaging electron energy of 42.5 eV which was commonly used in this work.

Island nucleation occurs with greatest probability where the adatom concentration is highest. This nucleation rate is commonly written as[15]

$$\omega \sim D n^{i^*+1}, \tag{1}$$

where D is the diffusion constant, n is the adatom concentration, and i^* is the critical nucleus size. Following the work of Burton, Cabrera, and Frank (BCF),[1] the adatom concentration on a terrace is governed by the diffusion equation subject to boundary conditions at steps

$$\frac{dn}{dt} = D\nabla^2 n + F - \frac{n}{\tau}, \tag{2}$$

where t is time, F is the incident atom flux, and τ is the adatom lifetime prior to desorption. In extension to the BCF theory, the following boundary conditions[16–19] are used here in one dimension appropriate for the geometry of the experiment:

$$D\left.\frac{dn}{dx}\right|_{\pm} = \pm K_{\pm}(n_{\pm}-n_{eq})+P(n_{\pm}-n_{\mp}), \tag{3}$$

where the concentration gradient is evaluated at the lower $(+)$ and upper $(-)$ sides of a step, K_+ and K_- are the kinetic coefficients for attachment from the lower and upper sides of a step, respectively, n_+ and n_- are the corresponding concentrations, n_{eq} is the equalibrium contration, and P is the kinetic coefficient describing step permeability. The general solution of Eq. (2) can be written as

$$n = F\tau + A\cosh\frac{x}{x_s} + B\sinh\frac{x}{x_s}, \tag{4}$$

where $x_s=\sqrt{D\tau}$ is the diffusion length prior to desorption. An important assumption will be made below that steps are equally spaced. The concentration profile and n_+ and n_- are then the same on each terrace and the boundary conditions in Eq. (3) can be applied at the steps that bound a single terrace. This use of boundary conditions is also permissible when steps are impermeable, without invoking the assumption of equally spaced step. The validity of this treatment in regards to the experimental data presented here will become apparent below.

Experimental measurements actually provide a distribution of nucleation positions. The distribution can be predicted by the nucleation rate [Eq. (1)] in conjunction with solution for the concentration [Eq. (4)]. Explicit expressions for the coefficients A and B in Eq. (4) are found by solving the simultaneous equations in A and B that are obtained from evaluation of the boundary conditions in Eq. (3),

$$A = \frac{-F\tau\left[(x_s^+ + x_s^-)\cosh\tilde{\lambda} + 2\left(x_s^+x_s^- + \frac{p}{\tilde{\lambda}}(x_s^+ + x_s^-)\right)\sinh\tilde{\lambda}\right]}{(x_s^+ + x_s^-)\cosh 2\tilde{\lambda} + \left[1 + x_s^+x_s^- + \frac{p}{\tilde{\lambda}}(x_s^+ + x_s^-)\right]\sinh 2\tilde{\lambda}}, \tag{5a}$$

$$B = \frac{F\tau(x_s^+ - x_s^-)\sinh\tilde{\lambda}}{(x_s^+ + x_s^-)\cosh 2\tilde{\lambda} + \left[1 + x_s^+x_s^- + \frac{p}{\tilde{\lambda}}(x_s^+ + x_s^-)\right]\sinh 2\tilde{\lambda}}, \tag{5b}$$

in terms of dimensionless quantities $p=P\lambda/D$, $\tilde{\lambda}=\lambda/2x_s$, $x_s^{\pm}=x_s/d_{\pm}$, where λ is the terrace width and $d_{\pm}=D/K_{\pm}$ is the kinetic length[3] that describes the relative importance of diffusion and step attachment processes, i.e., the rate limiting step. These expressions have an expected form with regards to the step attachment asymmetry. Asymmetry with respect to the midpoint of the terrace $x=0$ is introduced to the concentration $B\neq 0$ when $d_+\neq d_-$.

In order to demonstrate the importance of the kinetic length and permeability, we consider a hypothetical system with asymmetry, $d_+/d_->1$. Plotted in Fig. 1 for this hypothetical system is the ratio of the coefficients B/A as functions of the kinetic length and permeability. In the case that steps are impermeable [Fig. 1(a)], $P/D=0$, the ratio B/A is largest and the concentration is most asymmetric when the kinetic lengths are large, that is, in the ADL regime as would be expected. Conversely, the concentration becomes more symmetric when the kinetic lengths become smaller as the DL regime is approached. In the extreme DL case, $d_{\pm} \ll x_s$, A and B simplify to $1/\cosh(\lambda/2x_s)$ and 0, respectively, which reproduces the symmetric BCF result.[1] The impact of permeability is shown in Fig. 1(b). The left-hand side of this figure (for $P/D=0$) reproduces the right-hand side of Fig. 1(a). As the permeability is increased, the ratio of B/A is diminished and the concentration becomes more symmetric. This can be understood as follows. When the permeability is zero, then steps isolate the concentrations on adjacent terraces and a concentration difference across a step, i.e., $n_{\pm}-n_{\mp}$ in Eq. (3), can exist. In the limit of high permeability,

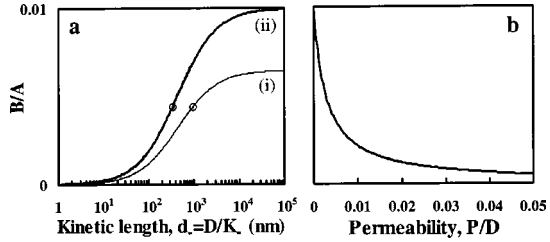

FIG. 1. Ratio of B/A [Eqs. (5a) and (5b)] vs (a) kinetic length and (b) permeability. In (a), curves are shown for asymmetry (i) $d_+/d_-=1.14$ and (ii) 1.22 corresponding to the cases of $i^*=98$ and 49, respectively. The circled data points in (a) correspond to kinetic lengths determined for these two values of i^*. The curve in (b) is for $d_+/d_-=1.22$.

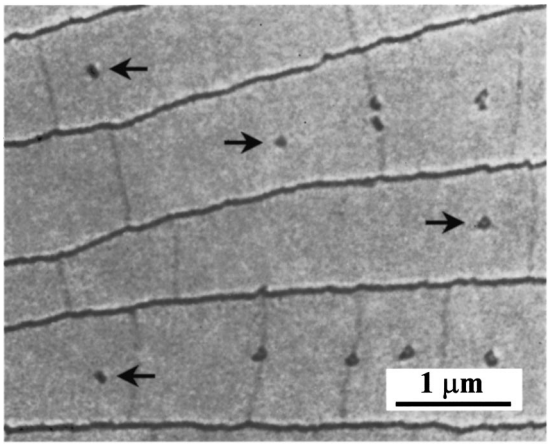

FIG. 2. LEEM image of the transition between step flow and two-dimensional nucleation and growth on the Si(111) (7×7) surface at 800 K. Islands at the critical terrace width are indicated by arrows. Dark lines are atomic steps. The step descending direction is from the bottom to top of the image. The imaging energy was 42.5 eV.

the concentrations across a step become nearly equal $n_+ \approx n_-$, which imposes symmetry on the concentrations on the terraces. Liu and Weeks have also pointed out the importance of step permeability in the context of electromigration-induced asymmetry.[20] In summary, DL processes and step permeability suppress asymmetry in the concentration profile and consequently step attachment asymmetry becomes irrelevant. There will be no current asymmetry to a step and step flow instabilities will not be realized. Simple interpretation of island nucleation position or denuded zones without due consideration given to the rate-limiting step, i.e., kinetic length, and step permeability can yield misleading results.

A few examples of islands at the critical terrace width for step flow are shown in Fig. 2 for growth at 800 K with an incident flux of 0.015 ML/min. The faint lines in this image that run perpendicular to step edges are domain walls. This domain boundary configuration is not expected to necessitate a two-dimensional model. The critical terrace width for step

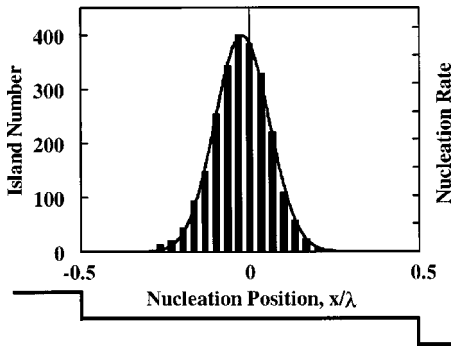

FIG. 3. Histogram of the island nucleation position relative to the step-up and step-down sides of a terrace of critical terrace width λ_c for step flow. For growth at 800 K, the peak position is $x_m/\lambda_c = -0.022 \pm 0.003$. The histogram bin size is $\Delta x/\lambda = 0.033$. The nucleation rate given by Eqs. (1), (4), and (5) is also shown (solid line). The step convention is shown below.

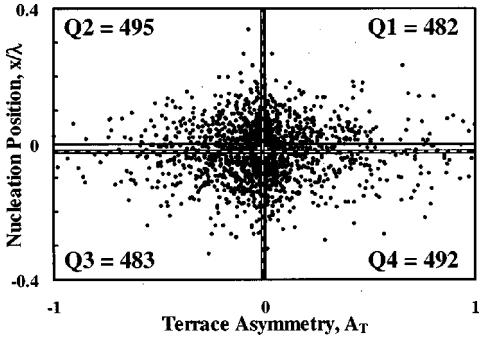

FIG. 4. Nucleation position vs terrace asymmetry factor A_T [Eq. (6)]. The number of data points in the four quadrants defined by the average values of nucleation position and A_T (distinguished by dashed axes) are indicated.

flow λ_c was equal to 950 ± 80 nm under these growth conditions. Figure 3 shows the full distribution of island number versus position. The distribution is shifted towards the step-up side and the maximum position is located at $x_m/\lambda_c = -0.022 \pm 0.003$.

Before reaching any conclusion about step attachment, however, it is important to consider other factors that may also produce a shift of the island position in this type of measurement. First of all, the measured island position is offset from the true nucleation position by an amount that is equal to the distance travelled by steps after nucleation. This spurious contribution was minimized in our work by arresting deposition immediately after islands were first detected with real-time LEEM imaging during growth. A total of $\theta = 0.010 - 0.020$ ML was deposited from the start to the finish in the different experiments. Taking the extreme view that nucleation occurs immediately at the start of deposition but goes undetected by LEEM for a while, a corresponding amount of step advancement, $\delta x/\lambda = \theta$, has been accounted for already by offsetting the coordinates of the nucleation positions in Fig. 3.

If steps are permeable, then the concentration on a given terrace will depend upon the widths of the adjacent terraces. The concentration on wider terraces is higher due to the larger capture area. Permeability allows a net adatom current to flow from wide to narrow neighboring terrace. This will bias the concentration on a given terrace towards (away from) its wider (narrower) neighboring terraces. As a consequence, the island nucleation position may be influenced if steps are not equally spaced and if they are permeable. In order to check for this, we have also measured the widths of the adjacent leading and trailing terrace, λ_{lead} and λ_{trail}, respectively. In Fig. 4, the nucleation position is plotted against the quantity that we call the terrace asymmetry factor A_T

$$A_T = \frac{\lambda_{\text{lead}} - \lambda_{\text{trail}}}{\lambda_c^2} \sqrt{(\lambda_{\text{lead}} - \lambda_c)^2 + (\lambda_{\text{trail}} - \lambda_c)^2}, \qquad (6)$$

where λ_c refers to the width of the terrace on which island nucleation occurs. The numerator of the first factor in Eq. (6) expresses that to first order the center-of-mass of the concentration on a terrace will be shifted towards the step-up (trail-

ing) side or step-down (leading) side depending upon the difference of the adjacent terrace widths. The factor in the square root reflects the fact that the concentration on a terrace of width λ_c will be more strongly influenced by permeability when the adjacent terrace widths are much larger or much smaller.

Figure 4 may be interpreted by examining the distribution of the data points. For impermeable steps and no step attachment asymmetry, the data points should be distributed isotropically about the point on the x axis that corresponds to the average value of A_T. If steps are permeable, then the data points will tend to be clustered in the first and third quadrants relative to the point defined by the average values of A_T and nucleation position, here -7.1×10^{-3} and -0.022, respectively. However, the number of points in these four quadrants in Fig. 4, $Q1=482$, $Q2=495$, $Q3=483$, $Q4=492$, are well within the $\sqrt{N}$ uncertainty of counting statistics. No clustering of data points in the first and third quadrant is detected. This result indicates either that steps are impermeable or that their permeability is insufficient to influence the island nucleation position perceptibly. Thus, we will take permeability $P=0$ in the following analysis. This leads to the conclusion that the results in Fig. 3 indicate an asymmetric adatom concentration and therefore that step attachment is favored from the terrace trailing an advancing step $K_- > K_+$ $(d_+ > d_-)$.

It can be shown that the value of K_-/K_+ that is determined with Eq. (5) from the nucleation data increases sharply at very short diffusion length, but approaches the asymptotic value for long diffusion lengths within 0.5% already by $x_s/\lambda=1$ for all values of the kinetic length.[21] It was also determined from real-time measurements of step flow velocity as a function of terrace width that $x_s>\lambda_c$ under the growth conditions used here.[21] Since desorption is negligible at the experimental temperature, the diffusion length is probably much longer. It is also apparent that the determination of K_-/K_+ depends upon the kinetic regime (DL vs ADL), which is characterized by the magnitude of the kinetic length [e.g., see Fig. 1(a)]. Knowledge of the kinetic length is therefore crucial.

Fitting of the full nucleation distribution with Eq. (1) in conjunction with Eqs. (4) and (5) can provide information about the kinetic length and kinetic coefficient asymmetry. In an atomistic picture, A and B can be expressed in terms of microscopic quantities. The kinetic lengths are given by

$$d_\pm = \frac{D}{K_\pm} = a\left(\frac{\nu_{\rm dif}}{\nu_\pm}\right)\exp(W_{\rm ES}^\pm/kT),$$

where $a=0.384$ nm, $W_{\rm ES}^+$ and $W_{\rm ES}^-$ are the Ehrlich-Schwoebel (ES) and anti-ES barriers, respectively, and $\nu_{\rm dif}$ and ν_- (ν_+) are the attempt frequencies for diffusive motion on a terrace and at the upper (lower) step edge, respectively. The desorption time is the inverse of the desorption rate $\tau = \nu_{\rm des}^{-1}\exp(E_{\rm des}/kT)$, where $\nu_{\rm des}$ and $E_{\rm des}$ are the attempt frequency and activation energy for desorption, respectively. The diffusion length is therefore related to diffusion and desorption processes according to

$$x_s = a(\nu_{\rm dif}/\nu_{\rm des})^{1/2}\exp\left(\frac{E_{\rm des}-E_{\rm dif}}{2kT}\right).$$

The attempt frequencies and activation energies that are used to fit the nucleation position must give a diffusion length which is greater than the critical terrace width $x_s>\lambda_c$, a condition that is dictated by experimental results (see above). Furthermore, asymptotic behavior for long diffusion length ($x_s \gg \lambda_c$) is already nearly obtained for the condition $x_s=\lambda_c$. The determination of the kinetic length is rather insensitive to the choice of attempt frequencies and activation energies as long as the condition $x_s>\lambda_c$ is respected in the analysis. We take $\nu_{\rm des}=\nu_{\rm dif}=10^{13}$ s^{-1} and $E_{\rm des}-E_{\rm dif}=1.3$ eV, which yields $x_s/\lambda_c\sim5$. Previously reported values of $E_{\rm dif}$ fall in the range 0.75 (Ref. 10) to 1.3 eV (Ref. 22). The smallest island that was observed with scanning tunneling microscopy during growth was one unit cell.[23] This places an upper limit of $i^*=98$ on the critical island size. The fit to the data shown in Fig. 3 was obtained for $i^*=98$ with $d_-=9.1\times10^2$ nm and $d_+/d_-=1.14$, which are upper limit and lower limit for the kinetic length and kinetic coefficient asymmetry, respectively. Equally good fits to the data were obtained for $i^*=49$, corresponding to one half (7×7) unit cell, with $d_-=3.3\times10^2$ nm and $d_+/d_-=1.22$, and an even smaller subunit $i^*=25$ with $d_-=61$ nm and $d_+/d_-=1.81$. Examining Fig. 1, the limiting condition on the kinetic length ($d_-=9.1\times10^2$ nm) is definitely not the ADL kinetic regime that has been claimed in Refs. 11 and 12, but lies intermediate between ADL and DL regimes.

Finally, it is necessary to make a comment about the equilibrium concentration, n_{eq}, which has been implicitly assumed to be zero. Inclusion of a nonzero equilibrium concentration in the analysis would lead to determination of smaller kinetic lengths, larger step attachment asymmetry, and consequently to the conclusion that growth tends more towards DL than with zero equilibrium concentration. Furthermore, the sensitivity of the measurement shown in Fig. 4 to permeability would be diminished. Previously, differences between the (7×7) surface and the disordered "(1×1)" surface at high temperature were accounted for well with the assumption that the equilibrium adatom concentration on the (7×7) is zero.[24] The equilibrium concentration on the Si(111) (7×7) surface is otherwise unknown and is an important topic for future work.

We are grateful to T. L. Einstein for providing valuable comments on the manuscript. This work was supported by the Hong Kong Research Grant Council under Grant No. HKUST6128/97P.

*Email address: phaltman@ust.hk

[1] W. K. Burton, N. Cabrera, and F. C. Frank, Philos. Trans. R. Soc. London, Ser. A **243**, 299 (1951).

[2] R. L. Schwoebel and E. J. Shipsey, J. Appl. Phys. **37**, 3682 (1966); R. L. Schwoebel, *ibid.* **40**, 614 (1969).

[3] G. S. Bales and A. Zangwill, Phys. Rev. B **41**, 5500 (1990).

[4] M. Uwaha and Y. Saito, Phys. Rev. Lett. **68**, 224 (1992).
[5] I. Bena, C. Misbah, and A. Valence, Phys. Rev. B **47**, 7408 (1993).
[6] A. Pimpenelli *et al.*, J. Phys. C **6**, 2661 (1994).
[7] M. D. Johnson *et al.*, Phys. Rev. Lett. **72**, 116 (1994).
[8] D. Kandel and J. Weeks, Phys. Rev. Lett. **69**, 3758 (1992).
[9] G. Ehrlich and F. Dudda, J. Chem. Phys. **44**, 1039 (1966).
[10] B. Voigtländer *et al.*, Phys. Rev. B **51**, 7583 (1995).
[11] A. Ichimiya, Y. Tanaka, and K. Ishiyama, Phys. Rev. Lett. **76**, 4721 (1996).
[12] A. Ichimiya, K. Hayashi, E. D. Williams, T. L. Einstein, M. Uwaha, and K. Watanabe, Phys. Rev. Lett. **84**, 3662 (2000).
[13] E. Bauer, Rep. Prog. Phys. **57**, 895 (1994).
[14] W. F. Chung and M. S. Altman, Ultramicroscopy **74**, 237 (1998).
[15] J. A. Venables *et al.*, Rep. Prog. Phys. **47**, 399 (1984).
[16] A. A. Chernov, Sov. Phys. Usp. **4**, 116 (1961).
[17] R. Ghez and S. S. Iyer, IBM J. Res. Dev. **32**, 804 (1988).
[18] S. Stoyanov, Europhys. Lett. **11**, 361 (1990).
[19] M. Ozdemir and A. Zangwill, Phys. Rev. B **45**, 3718 (1992).
[20] Da-Jiang Liu and John D. Weeks, Phys. Rev. B **57**, 14 891 (1998).
[21] W. F. Chung and M. S. Altman (unpublished).
[22] A. V. Latyshev, A. B. Krasilnikov, and A. L. Aseev, Phys. Rev. B **54**, 2586 (1996), and references therein.
[23] Bert Voigtländer, Martin Kaestner, and Pavel Smilauer, Phys. Rev. Lett. **81**, 858 (1998).
[24] Y. N. Yang and E. D. Williams, Phys. Rev. Lett. **72**, 1862 (1994).